JOURNAL OF AIRCRAFT
Vol. 30, No. 5, Sept.–Oct. 1993

Envelope Function—A Tool for Analyzing Flutter Data

J. E. Cooper,* P. R. Emmett,† and J. R. Wright*
University of Manchester, Manchester M13 9PL, England, United Kingdom
and
M. J. Schofield‡
British Aerospace (Commerical Aircraft), Ltd., Hatfield AL10 9TL, England, United Kingdom

In this article a new tool for flutter clearance is presented and a preliminary assessment of its capabilities undertaken. It is intended to be complementary to other approaches. The method is based on quantifying the change in the shape of the decay envelope associated with control pulse responses or impulse response functions. An indication of overall stability is obtained without curve fitting by way of a shape parameter which quickly shows whether there has been any significant change since the last test point. In addition, the envelope functions can be overlayed from different speeds. The method is illustrated with data from a simulated aeroelastic model of a multiengined transport aircraft, and the effects of turbulence are considered. Finally, the method is successfully applied to real flight test data.

I. Introduction

FLIGHT flutter tests are carried out on prototype versions of new or significantly modified commercial and military aircraft in order to demonstrate freedom from flutter over the entire flight envelope. Often substantial wind-tunnel flutter testing is also carried out. Flutter clearance can be very costly and time-consuming, and proceeding to the next speed or Mach number is not without some risk, given the complexity of the flutter phenomenon and data corrupted by the response due to turbulence, etc.

At each test point the clearance process is usually to measure the dynamic response of the aircraft to a control pulse (or "jerk"), to a deliberately imposed excitation such as a chirp by way of the control surface or an inertial exciter, or to the natural turbulence excitation. An adequate level of stability may initially be assessed by a subjective visual inspection of time histories, but often the measured data are used to obtain frequencies and dampings of the "modes" present by means of some form of curve fitting. Trends of the variation of frequency and damping with speed or Mach number for each mode are then observed in order to see if the damping is likely to become significantly smaller before the next test point. The curve-fitting process can be extremely difficult, particularly if the signal-to-noise ratio is poor and/or there are modes with very closely spaced frequencies as on an aircraft with multiple engines or stores. Thus, while the use of trends is objective, the quality of results can occasionally mean that some subjectivity can creep into the clearance decision.[1,2]

Since considerable weight is often placed upon visual inspection of time histories, and since sometimes only control jerk responses are available (as when testing an aircraft variant), it would perhaps be useful to have a somewhat more objective measure of the stability associated with a particular time record.

In this article a new tool for flutter clearance is proposed to complement existing approaches. The aim is to compare the envelopes of time decays as speed or Mach number is increased by inspection and by way of a simple stability parameter. Many transducer responses could be considered quickly prior to any attempt at curve fitting and a "feel" for any change in overall stability gained. A further application of the technique may be the analysis of aeroelastic transients calculated by many computational fluid dynamics (CFD) codes.

Received Oct. 17, 1991; revision received July 27, 1992; accepted for publication July 31, 1992.

*Lecturer, Department of Engineering, Oxford Rd.
†Research Assistant, Department of Engineering, Oxford Rd.
‡Structural Dynamics Manager, Aerodynamics Department, Airlines Division, Comet Way.

II. Obtaining the Decay Envelope

Given a decaying response which is the superposition of a number of damped sinusoids, the obvious way of obtaining the envelope of the decay is to search for successive maxima and minima and to join up the peaks and the troughs. This process only gives discrete values on the envelope which is disadvantageous if the decay has very few cycles. Also, a lot of small local peaks due to the presence of high-frequency noise can obscure what is happening.

An alternative approach is to construct the envelope function using the Hilbert transform,[3–5] which allows a signal to be generated for which every component is in quadrature with the measured decay at all frequencies within the measurement range. Let the measured decay by $y(t)$ and let the Fourier transform of $y(t)$ be $Y(i\omega)$, so that

$$Y(i\omega) = F[y(t)] = Y_R + iY_I \tag{1}$$

where $F[\ ]$ denotes the Fourier transform. Now the Hilbert transform $y_H(t)$ may be defined in the time domain as

$$y_H(t) = \frac{1}{\pi}\int_{-\infty}^{+\infty} \frac{y(\tau)}{t-\tau}\,\mathrm{d}\tau \tag{2}$$

or

$$y_H(t) = y(t)^*(1/\pi t) \tag{3}$$

where * indicates a convolution in time. Noting that

$$F(1/\pi t) = -i\ \mathrm{sgn}\ \omega \tag{4}$$

where $\mathrm{sgn}\ \omega = +1(\omega > 0)$ or $-1(\omega < 0)$, then the convolution may be expressed as a frequency domain multiplication, namely

$$F[y_H(t)] = F[y(t)]F(1/\pi t) = Y(i\omega)(-i\ \mathrm{sgn}\ \omega) \tag{5}$$

Thus

$$y_H(t) = F^{-1}[Y(i\omega)(-i\ \mathrm{sgn}\ \omega)] \tag{6}$$

where F^{-1} is the inverse Fourier transform. It is most straightforward to obtain $y_H(t)$ by way of the frequency domain, noting that for $\omega > 0$ then Eq. (6) becomes

$$y_H(t) = F^{-1}(Y_I - iY_R) \tag{7}$$

At $\omega = 0$, the frequency domain function is constrained to be real, so effectively, sgn $\omega = 0$ at $\omega = 0$. Thus, a simple transform, rearrangement, and inverse transform will yield $y_H(t)$, a signal whose frequency components differ from those in $y(t)$ by 90 deg in phase. If, for example, a single degree-of-freedom decay is

$$y(t) = Ae^{-\sigma t} \sin \omega_d t$$

where σ is the decay rate and ω_d the damped natural frequency, then it may be shown analytically that for small damping

$$y_H(t) = -Ae^{-\sigma t} \cos \omega_d t$$

Now consider forming a complex time function as

$$\hat{y}(t) = y(t) + iy_H(t) \tag{8}$$

where the modulus of this function

$$|\hat{y}(t)| = [y(t)^2 + y_H(t)^2]^{1/2} = \text{env}(t) \tag{9}$$

may be called the "envelope" function. For the simple example

$$\text{env}(t) = Ae^{-\sigma t}$$

which is clearly the envelope of the decay and indicates damping (or stability). For a more general multi-degree-of-freedom decay then env(t) is the decay envelope, and will provide an indication of the general stability of the system.

As an example, in Figs. 1–3 the $y(t)$, $y_H(t)$, and env(t) are presented for a single degree-of-freedom system with a natural frequency of 10 Hz and a damping of 1% critical; the data were generated digitally. The envelope function is a simple exponential decay as expected.

Now it may be argued that the envelope is easier to inspect and absorb than the entire oscillatory decay, although the envelope is more complicated for multi-degree-of-freedom systems where "beating" occurs. Clearly one way of observing the change in stability from one flight speed to another is to overlay envelope functions from each speed for particular transducers. A tendency for the envelope decay to be prolonged will probably indicate a decrease in damping.

One problem with simple overlaying of envelopes is that the decays may have different overall amplitudes due to different strength jerks. If $y(t)$ were the time impulse response function derived from the frequency response function $Y(i\omega)$ rather than a control jerk response, then variability in excitation levels would be accounted for, but the decay magnitudes could still change due to different aerodynamic effects.

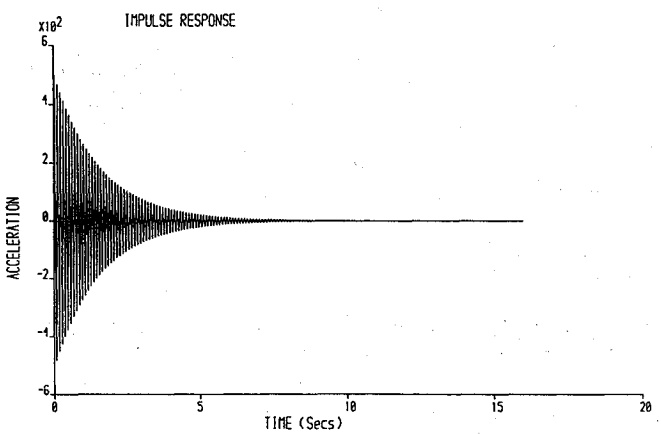

Fig. 1 Single degree-of-freedom impulse response.

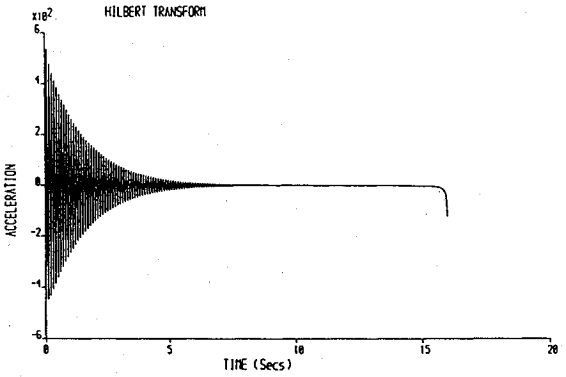

Fig. 2 Single degree-of-freedom Hilbert transform.

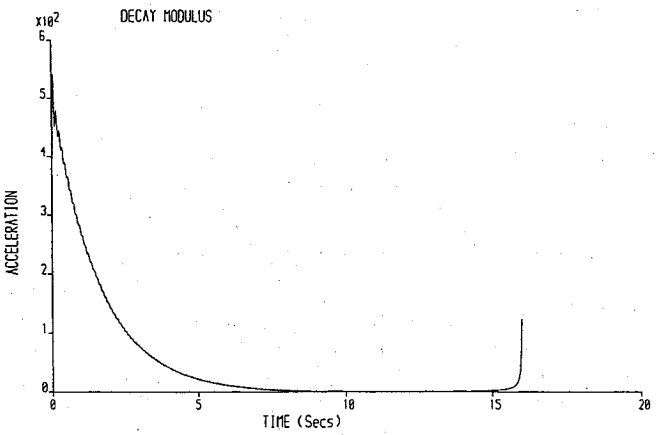

Fig. 3 Single degree-of-freedom envelope function.

III. Shape Parameters for the Decay Envelope

One possible solution to the problem of varying decay amplitudes is to consider changes in the shape of the envelope function, irrespective of overall amplitude.

If the envelope is considered to enclose an area between it and the time axis, then the properties of this area will provide information about the shape of the envelope. A prolonging of the decay, as would happen for lower damping, would be indicated by an increase in the distance of the centroid of the area from the amplitude axis, or indeed by an increase in the radius of gyration of the area about the amplitude axis.

Referring to Fig. 4, the time centroid may be defined as

$$\bar{t}_1 = \left[\int_0^{t_{\max}} \text{env}(t) \cdot t \, dt \Big/ \int_0^{t_{\max}} \text{env}(t) \, dt \right] \tag{10}$$

and the time radius of gyration by

$$\bar{t}_2 = \left[\int_0^{t_{\max}} \text{env}(t) \cdot t^2 \, dt \Big/ \int_0^{t_{\max}} \text{env}(t) \, dt \right]^{1/2} \tag{11}$$

where $t_{\max}$ is the maximum value of time chosen to give an upper bound to the enclosed area. This maximum value would need to be the same for all tests for each given transducer.

Now, for the analytical single degree-of-freedom example considered earlier

$$\text{env}(t) = Ae^{-\sigma t}$$

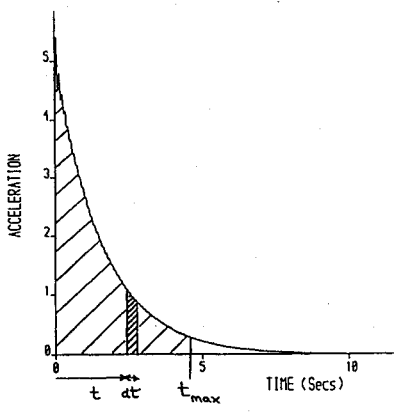

Fig. 4 Envelope function.

and it can be shown that for $t_{max} = \infty$ then

$$\bar{t}_1 = (1/\sigma), \qquad \bar{t}_2 = (1.414/\sigma)$$

where σ is the decay rate. The results are more involved for $t_{max} < \infty$.

Since $\bar{t}_1$ and $\bar{t}_2$ will increase as damping decreases, it was considered better to use the inverse of these values to give a measure of the shape of the envelope. Experience has indicated that the behavior of $1/\bar{t}_2$ as damping is reduced is not as smooth as $1/\bar{t}_1$ for finite t_{max}; also the radius of gyration will tend to give larger weighting to the envelope data at large values of t, where the signal-to-noise ratio for the envelope will be poorer.

Thus, a shape parameter may be defined as

$$S = (1/\bar{t}_1) \tag{12}$$

and a decrease in S will indicate a decrease in system damping. For a single degree-of-freedom system, it may be shown that when the damping becomes zero then S becomes $2/t_{max}$, therefore giving a threshold for instability. However, for multi-degree-of-freedom (DOF), the situation is less clear cut, and a damping tending to zero will reduce S rapidly, but not to the value $2/t_{max}$ because of the effect of other damped modes. Extrapolation to a precise flutter speed will not usually be possible; the envelope just provides a "quick look" tool which may indicate whether damping has changed significantly since the last test. Thus, S may be considered as a crude measure of the overall system damping.

Note that an estimate for $\bar{t}_1$, and therefore S, may be obtained very quickly from the raw time data without any transformation using

$$\bar{t}_1 \approx \left[\int_0^{t_{max}} t|y(t)|\,dt \Big/ \int_0^{t_{max}} |y(t)|\,dt \right] \tag{13}$$

IV. Simple Binary Flutter Example

In order to illustrate the envelope approach, impulse response data were generated for a two degree-of-freedom system whose frequencies and dampings were modified so as to match classical wing bending, torsion behavior.

The variation in damping with speed for the two modes is shown in Fig. 5. The variation in the shape parameter S with speed is shown in Fig. 6 for $t_{max} = 10$ s. Because the response is dominated by the flutter mode at the flutter speed, the condition of zero damping corresponds to $S = 2/t_{max} = 0.2$ as seen in the figure. Thus, the onset of the flutter condition was seen without any curve fitting or assumption as to the number of modes present.

V. Simulated Multiengined Aircraft Example

A mathematical model has been developed with the aim of simulating the aeroelastic behavior of a multiengined trans-

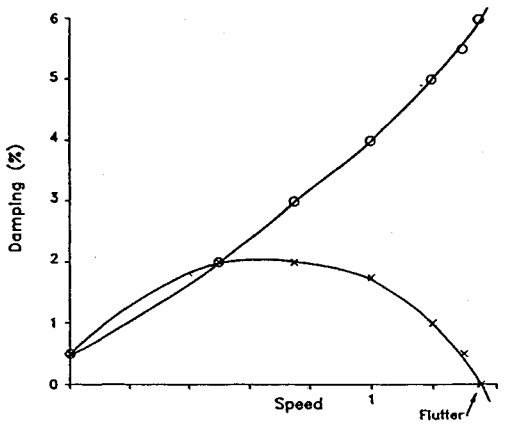

Fig. 5 Two degree-of-freedom flutter example. Variation of dampings with speed.

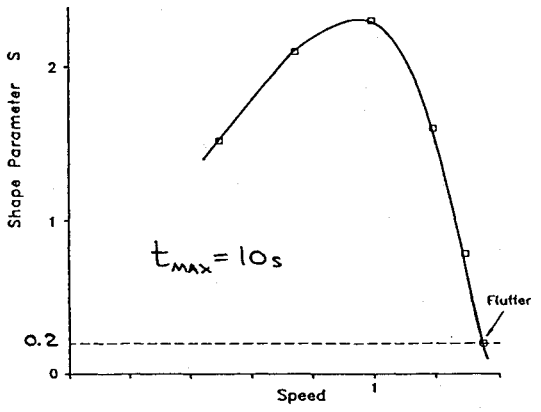

Fig. 6 Two degree-of-freedom flutter example. Variation of shape parameter with speed.

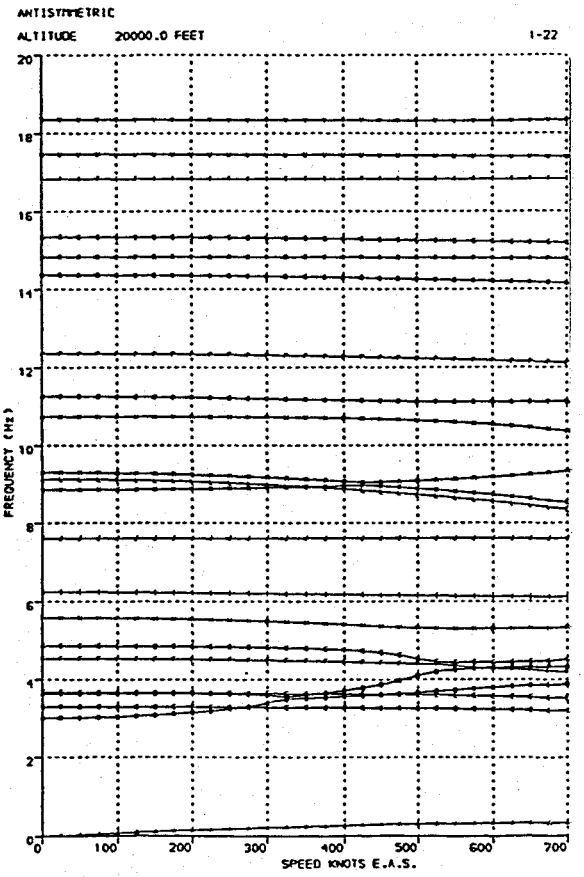

Fig. 7 Simulated multiengined aircraft example. Variation of frequencies with speed; antisymmetric.

port aircraft with an artifically low flutter speed. Symmetric or antisymmetric behavior may be considered, with about 20 modes in each model covering the range 0–20 Hz.

The variations in frequency and damping with speed for the antisymmetric model at 20,000 ft altitude are shown in Figs. 7 and 8. The flutter speed is 390 kt equivalent air speed (EAS) and the flutter mode around 4 Hz.

The model was excited on the wing with a frequency sweep from 2 to 20 Hz at 200, 250, 300, 350, 370, and 390 kt EAS, and the acceleration responses, transfer functions and impulse response functions obtained for the wing tip vertical and outboard engine lateral transducers. A sample transfer function and impulse response are presented in Figs. 9 and 10, respectively, for acceleration data.

The Hilbert transform and envelope function were then calculated, and the S evaluated for $t_{max} = 10$ s. A typical envelope function is shown in Fig. 11; the complicated behavior with multiple modes means that the function is not easy to interpret. Plots of shape parameter $S(=1/\bar{t}_1)$ against speed is shown for the wing tip transducer in Fig. 12. There is a clear drop in the parameter as flutter is approached but the actual flutter speed is not predicted; the "tool" simply flags a warning that the stability is reducing or alternatively indicates that nothing much has changed since the last speed.

The change in the envelope function is not very dramatic for the acceleration data. This is because the response is dominated by the higher frequency behavior and the lightly damped low-frequency mode is not very evident. However, by dividing the transfer function by $(i\omega)$ or $(-\omega^2)$ it is possible to convert the data to velocity or displacement form, respectively, thus enhancing the lower frequency contribution to the response as seen in Fig. 13 for displacement data. The corresponding

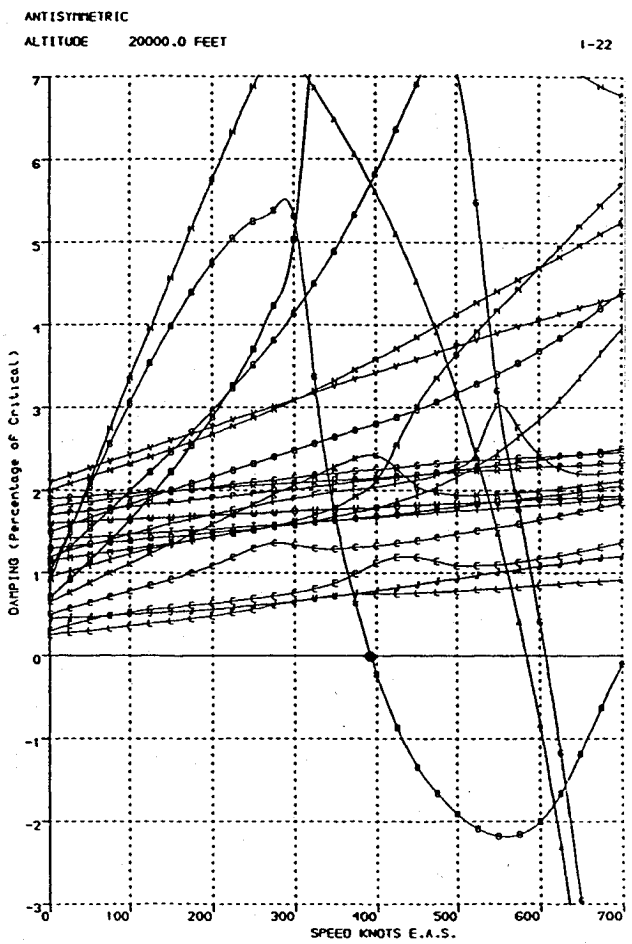

Fig. 8 Simulated multiengined aircraft example. Variation of dampings with speed; antisymmetric.

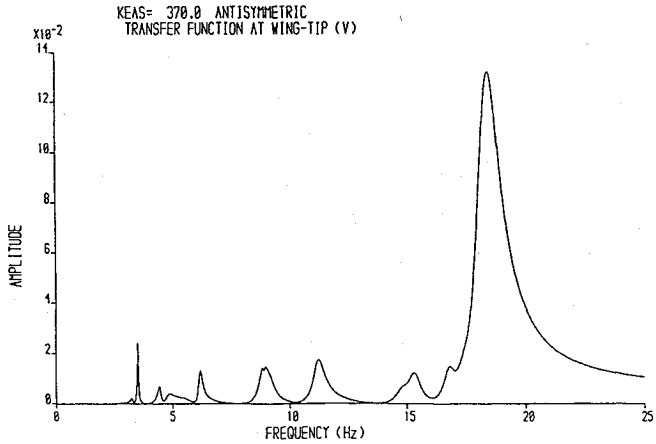

Fig. 9 Acceleration transfer function for wing tip at 370 kt.

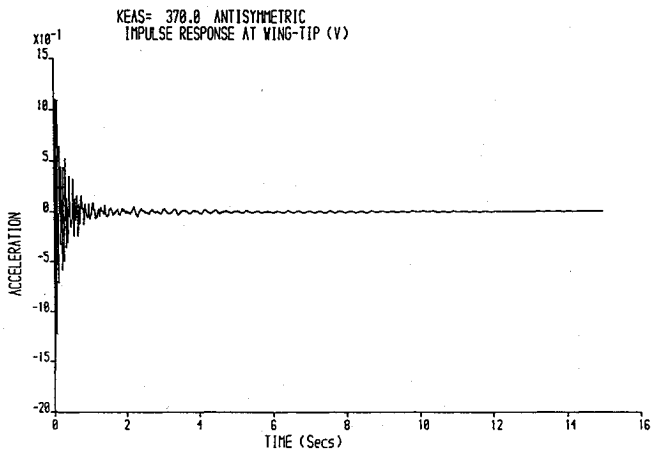

Fig. 10 Acceleration impulse response function for wing tip at 370 kt.

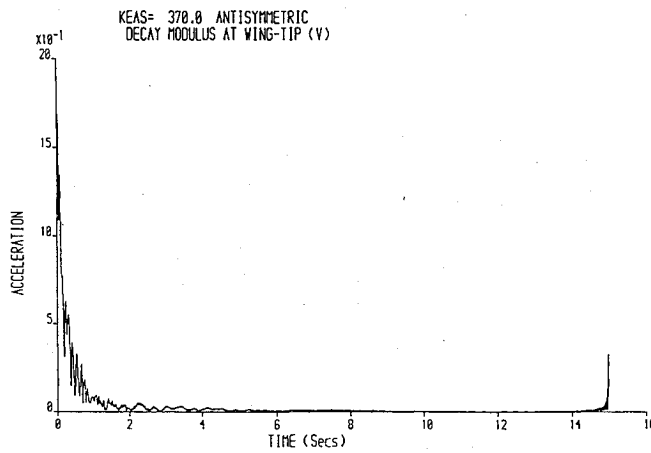

Fig. 11 Envelope function for wing tip acceleration at 370 kt.

shape parameter variation for displacement data is shown in Fig. 14. Note from the damping trends in Fig. 8 that no loss of stability is anticipated until nearly 400 kt, and the shape parameter plots in Figs. 12 and 14 both indicate flutter occurring at this speed.

If the flutter had occurred at a high frequency, use of the acceleration data would have been best. The stability over a particular bandwidth could be assessed by using a bandpass filter prior to calculation of the envelope function. Note that when using displacement data, care will have to be taken with rigid body responses, possibly using some form of high-pass filter.

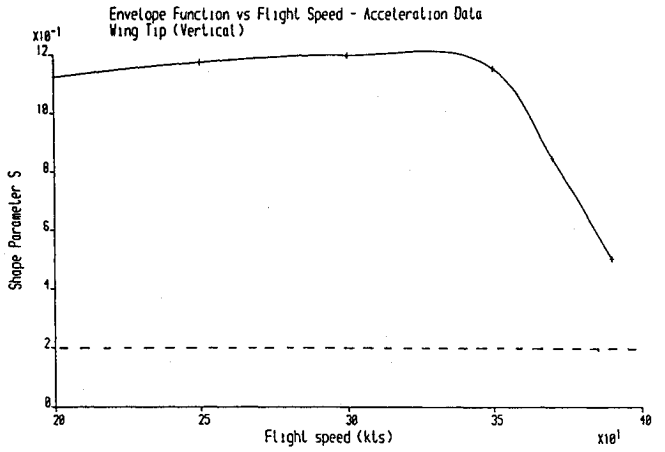

Fig. 12 Variation of shape parameters with speed for wing tip acceleration response.

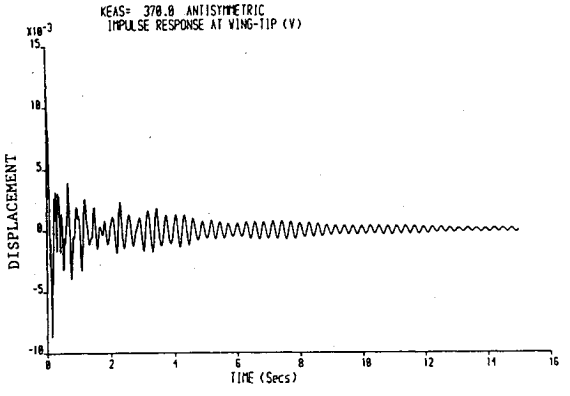

Fig. 13 Displacement impulse response function for wing tip at 370 kt.

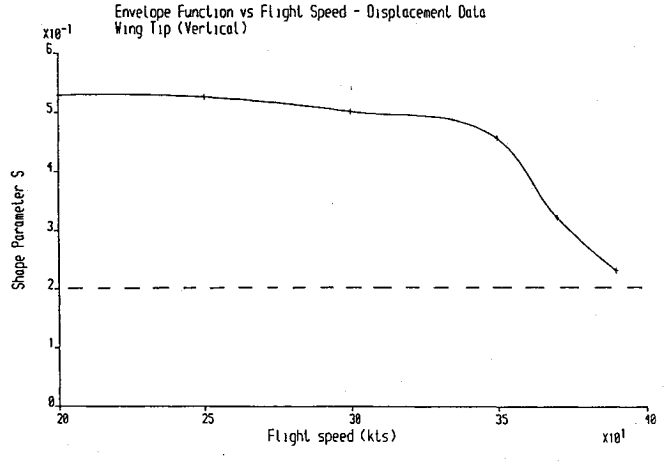

Fig. 14 Variation of shape parameter with speed for wing tip displacement response.

In practice, the envelope approach is most likely to be spoiled by the effects of the response to atmospheric turbulence on the decay data, and therefore, on the envelope function which would fluctuate due to the presence of noise. The value of t_{max} would need to be chosen carefully since the calculation of the centroid value $\bar{t}_1$ tends to weight the response at higher values of time where the signal-to-noise ratio is poorer; the effect on $\bar{t}_2$ would be more severe.

A preliminary assessment on the likely effects of turbulence has been carried out by obtaining the response of the model to random turbulence at the position of interest and adding it to the noise-free data, therefore producing noise-corrupted impulse response functions.

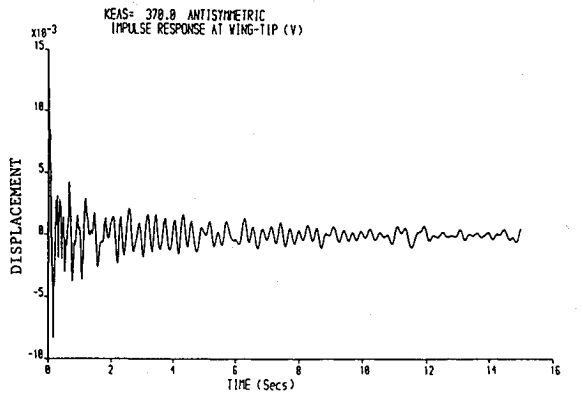

Fig. 15 Displacement impulse response function (plus turbulence) for wing tip at 370 kt.

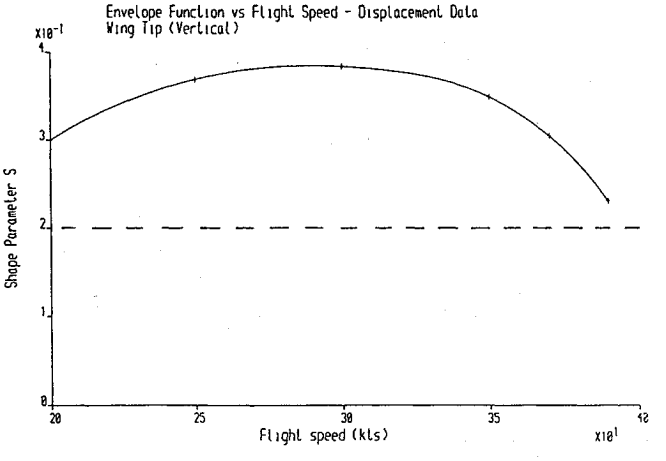

Fig. 16 Variation of shape parameter with speed for wing tip displacement response (plus turbulence).

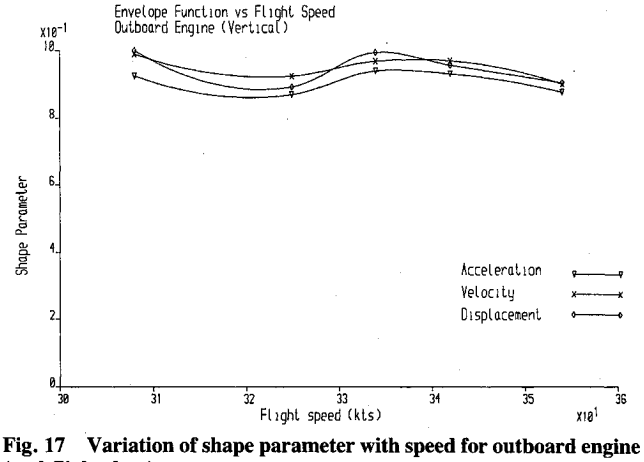

Fig. 17 Variation of shape parameter with speed for outboard engine (real flight data).

A typical noisy displacement response is shown in Fig. 15. The noise is primarily at very low frequency because of the ω^2 filter effect. The variation in shape parameter is shown in Fig. 16. When compared to the noise-free result in Fig. 14, the parameter values are smaller at lower speeds where the noise extends the envelope, but much the same at higher speeds; this is because the peaks and troughs introduced by the noise into the envelope tend to average out. The parameter curve is thus flatter, though the drop at flutter is still evident. The effectiveness of the method clearly depends on the level of noise and the value of t_{max}; reducing t_{max} too much tended also to flatten the shape parameter variation.

A possible way of reducing the effect of noise would be to apply some exponential weighting to the envelope function

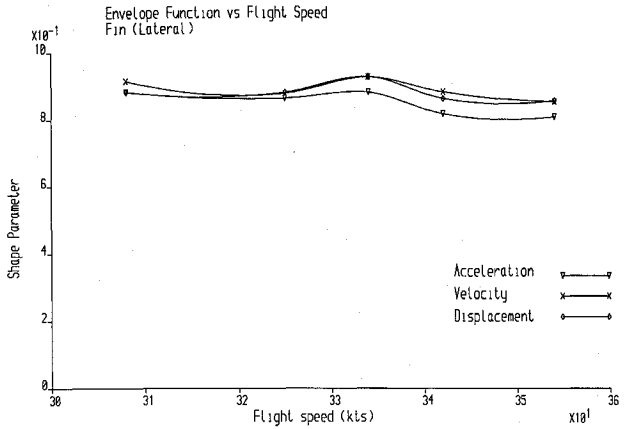

Fig. 18 Variation of shape parameter with speed for fin lateral (real flight data).

for all transducers and at all speeds, prior to evaluating the shape parameter. (Note that if using control jerk response data, the position of $t = 0$ needs to be chosen consistently throughout the sequence of flutter tests.)

VI. Application to Flight Test Data

The envelope approach was applied to aileron stick jerk response data acquired from the flight test[6] of the BAe146-300 in which flutter clearance was primarily based on swept sine excitation. Figures 17 and 18 show values of the envelope function for acceleration, velocity, and displacement (the latter two obtained by division by $i\omega$ in the frequency domain) at two of the measurement stations for a number of airspeeds. It can be seen that the stability of the response remains essentially constant throughout the speed range.

Although there was a greater high-frequency turbulence corruption on the acceleration envelope than that on the velocity and displacement envelopes, no advantage seems to be gained in calculating the envelope function for the other responses. It would thus appear that as long as the level of high-frequency turbulence is not excessively high, then turbulence does not seem detrimental to the use of the envelope function.

VII. Conclusions

A new tool for flutter clearance has been developed. It is based on changes in the shape of the envelope, either for control jerk response data or for impulse response functions obtained by way of the transfer function. No curve-fitting or extra testing is required, and an overall feel for change of stability is obtained. Different strengths of pulse are allowed for.

The tool is not intended to replace existing methods, but rather to provide a quick indication of whether there has been any significant change in stability since the previous test point. Noise, as for all methods, makes the process less clear cut and needs further investigation, as does the effect of a high-frequency flutter. The method needs further evaluation on real flight or tunnel data.

Acknowledgment

This work was carried out under research contract funding from British Aerospace (Commerical Aircraft) Ltd, Airlines Division, Hatfield, to whom the authors are grateful for permission to publish this article.

References

[1]Sandford, M. C., Abel, I., and Gray, D. L., "Development and Demonstration of a Flutter Suppression System Using Active Controls," NASA-TR R-450, Dec. 1975.

[2]Doggett, R. V., Jr., "Some Observations on the Houbolt-Rainey and Peak-Hold Methods of Flutter Onset Prediction," NASA TM 102745, Nov. 1990.

[3]Thrane, N., "The Hilbert Transform," TR 3, Bruel and Kjaer, Naerum, Denmark, 1984.

[4]Agneni, A., and Balis Crema, L. "Damping Measurements from Truncated Signals via Hilbert Transforms," *Mechanical Systems and Signal Processing*, Vol. 3, Jan. 1989, pp. 1–13.

[5]Mohammed, K. S., and Tomlinson, G. R. "A Simple Method of Accurately Determining the Apparent Damping in Non-Linear Structures," *Proceedings of the 7th International Modal Analysis Conference*, Bethel, CT, 1989, pp. 1336–1346.

[6]Cooper, J. E., and Wright, J. R., "Application of Time Domain Decomposition Techniques to Aircraft Ground Vibration and Flutter Test Data," *European Forum on Aeroelasticity and Structural Dynamics*, Bonn, Germany, 1989, pp. 235–243.